Synthesis, Structural, Spectroscopic, and Alkali-Metal Cations Complexation Studies of a Bis-Anthracenediyl Macrotricyclic Ditopic Receptor

Frédéric Fages,* Jean-Pierre Desvergne, and Henri Bouas-Laurent

Laboratoire de Photochimie Organique, CNRS URA 348, 351 Cours de la Libération, 33405 Talence Cedex, France

Jean-Marie Lehn

Chimie Supramoléculaire, CNRS URA 422, Institut Le Bel, 4 Rue Blaise Pascal, 67000 Strasbourg, France

Yvette Barrans* and Pierre Marsau

Laboratoire de Cristallographie et de Physique Cristalline, CNRS URA 144, 351 Cours de la Libération, 33405 Talence Cedex, France

Michel Meyer and Anne-Marie Albrecht-Gary

Laboratoire de Physico-Chimie Bioinorganique, CNRS URA 405, EHICS, 67000 Strasbourg, France

Received November 24, 1993 (Revised Manuscript Received June 16, 1994®)

The macrotricyclic bis-anthracenediyl receptor **1** has been prepared in order to study the interplay between cation complexation and fluorescence emission. The structure of this photoresponsive supramolecular system is based on two diazacrown ether moieties (N_2O_4) linked through two anthracene chromophore-containing flexible spacers. **1** displays a dual (locally excited and excimer-type) fluorescence emission, and the relative contribution (Φ_{FE}/Φ_{FM}) of these emissions is sensitive to metal cations. A spectroscopic study shows that the optical responses are dependent on the nature of the complexed cation, and the more pronounced effect is noticed with Rb^+. X-ray crystallographic, photophysical, and binding studies confirm that two Rb^+ cations are held within the hydrophilic N_2O_4 parts with participation of the four phenolic oxygen atoms to complexation, leading to the maximum overlap between the anthracene nuclei in both the ground and excited states. The mononuclear and binuclear rubidium complexes exhibit high stability constants in solution ($K_1 = 6.0 \times 10^5\ M^{-1}$; $K_2 = 6.3 \times 10^4\ M^{-1}$) and a noncooperative behavior is observed. This new supramolecular system can thus be used for sensitive metal cation detection and recognition, especially for Rb^+.

The design and synthesis of photosensitive complexing molecules are actively pursued for the development of supramolecular photoactive devices.[1] In that connection, fluorescent receptors have been synthesized and are used as sensitive probes for the recognition and the determination of metal cations in solution.[2–5] Among those, anthracene-containing crown ethers and cryptands were shown to act not only as sensitive fluorescence-based indicators for metal cations detection,[4a,6,7] but also to be especially well suited for the study of oriented weak interactions between π clouds and heavy atoms such as Ag^+, Tl^+,[4h,6a,8] or Cd^{2+}.[9]

The bis-anthracenediyl macrotricyclic receptor **1** (Scheme 1) has been designed to combine the remarkable photophysical properties of two anthracene rings and the complexing ability of two N_2O_4 subunits toward either ammonium or alkali-metal cations. Indeed, this receptor of cylindrical shape belongs to a new class of photosensitive ligands that enable the detection of linear molecular diammonium substrates by fluorescence spectroscopy.[10] Moreover, a preliminary study[11] has demonstrated that **1** is able to form binuclear [3]-cryptates with rubidium

® Abstract published in *Advance ACS Abstracts,* August 1, 1994.

(1) *Frontiers in Supramolecular Organic Chemistry and Photochemistry*; Schneider, H. J., Dürr, H., Eds.; VCH: Weinheim, 1991.

(2) *Fiber Optic Chemical Sensors and Biosensors*; Wolfbeis, O. S., Ed.; CRC Press: Boca Raton, FL, 1991; Vols. I and II.

(3) *Fluorescent Chemosensors for Ion and Molecule Recognition*; Czarnik, A. W., Ed.; ACS Symposium Series No. 538; American Chemical Society: Washington, DC, 1992.

(4) (a) Bissel, R. A.; de Silva, A. P.; Gunaratne, H. Q. N.; Lynch, P. L. M.; Maguire, G. E. M.; Sandanayake, K. R. A. S. *Chem. Soc. Rev.* **1992**, 187. (b) Martin, M. M.; Plaza, P.; Dai Hung, N.; Meyer, Y. H.; Bourson, J.; Valeur, B. *Chem. Phys. Lett.* **1993**, *202*, 425. (c) Bourson, J.; Pouget, J.; Valeur, B. *J. Phys. Chem.* **1993**, *97*, 4552. (d) Löhr, H.-G.; Vögtle, F. *Acc. Chem. Res.* **1985**, *18*, 65. (e) Létard, J.-F.; Lapouyade, R.; Rettig, W. *Pure Appl. Chem.* **1993**, *65*, 1705. (f) Jin, T.; Ichikawa, K.; Koyama, T. *J. Chem. Soc., Chem. Commun.* **1992**, 499. (g) Aoki, I.; Sakaki, T.; Shinkai, S. *J. Chem. Soc., Chem. Commun.* **1992**, 730. (h) Fages, F.; Desvergne, J.-P.; Bouas-Laurent, H.; Marsau, P.; Lehn, J.-M.; Kotzyba-Hibert, F.; Albrecht-Gary, A.-M.; Al-Joubbeh, M. *J. Am. Chem. Soc.* **1989**, *111*, 8672.

(5) For applications of metal recognition-based fluorescent probes in biological media, see: (a) Grynkiewicz, G.; Poenie, M.; Tsien, R. Y. *J. Biol. Chem.* **1985**, *260*, 3440. (b) Minta, A.; Tsien, R. Y. *J. Biol. Chem.* **1989**, *264*, 19449. (c) Loyevsky, M.; Lytton, S. D.; Mester, B.; Libman, J.; Shanzer, A.; Cabantchik, Z. I. *J. Clin. Invest.* **1993**, *91*, 218 and references therein.

(6) (a) Desvergne, J.-P.; Fages, F.; Bouas-Laurent, H.; Marsau, P. *Pure Appl. Chem.* **1992**, *64*, 1231. (b) Bouas-Laurent, H.; Desvergne, J.-P.; Fages, F.; Marsau, P. In ref 3, chapter 5, and in ref 1, p 265.

(7) (a) Czarnik, A. W. In ref 2, p 109. (b) Huston, M. E.; Haider, K. W.; Czarnik, A. M. *J. Am. Chem. Soc.* **1988**, *110*, 4460. (c) Akkaya, E. U.; Huston, M. E.; Czarnik, A. W. *J. Am. Chem. Soc.* **1990**, *112*, 3590. (d) Chae, M.-Y.; Czarnik, A. W. *J. Am. Chem. Soc.* **1992**, *114*, 9704. (e) Pérez-Jiménez, C.; Harris, S. J.; Diamond, D. *J. Chem. Soc., Chem. Commun.* **1993**, 480.

(8) Fages, F.; Desvergne, J.-P.; Bouas-Laurent, H.; Hinschberger, J.; Marsau, P.; Pétraud, M. *New. J. Chem.* **1988**, *12*, 95.

(9) Huston, M. E.; Engleman, C.; Czarnik, A. W. *J. Am. Chem. Soc.* **1990**, *112*, 7054.

(10) Fages, F.; Desvergne, J.-P.; Kampke, K.; Bouas-Laurent, H.; Lehn, J.-M.; Meyer, M.; Albrecht-Gary, A.-M. *J. Am. Chem. Soc.* **1993**, *115*, 3658.

0022-3263/94/1959-5264$04.50/0

Scheme 1. Bis-Anthracenediyl Macrotricyclic Receptor 1, Schematic Structure of Its Binuclear Inclusion Complex with $RbClO_4$, and the Hypothetical Structure of Its Inclusion Complex with α,ω-Heptamethylenediammonium Dichloride[a]

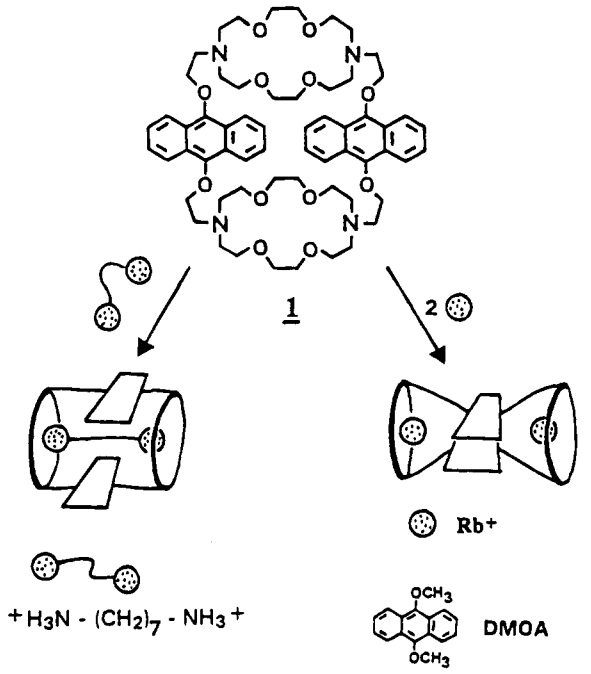

[a] 9,10-Dimethoxyanthracene (DMOA) is the monochromophoric reference molecule. (In our laboratories, **1** is termed "tonnelet" (small barrel).)

Scheme 2. The Bis-Anthracenediyl Cyclophanes *AAnn*[a]

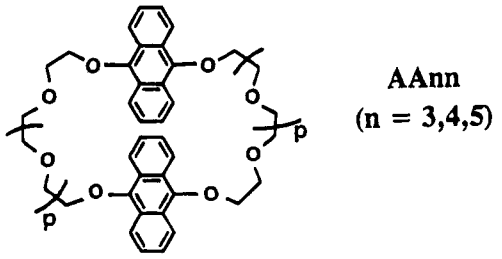

[a] *n* corresponds to the number of oxygen atoms in each crown-ether moiety; $n = p + 3$.

cations (Scheme 1) and that the fluorescence emission properties of **1** in solution are strongly altered upon complexation with a variety of cations, especially with Rb^+. This behavior is reminiscent of that of a macrocyclic bis-anthracenediyl cyclophane,[12] AA55, which displays light conversion (monomer to excimer fluorescence) in the presence of sodium cations (Scheme 2).

Here, we report the synthesis of compound **1**, a study of the complexation and photophysical properties of that receptor in the presence of alkali-metal cations (with emphasis on Rb^+), and the crystal structure of free **1** and of its dinuclear rubidium [3]-cryptate.

Scheme 3. Synthesis of receptor 1[a]

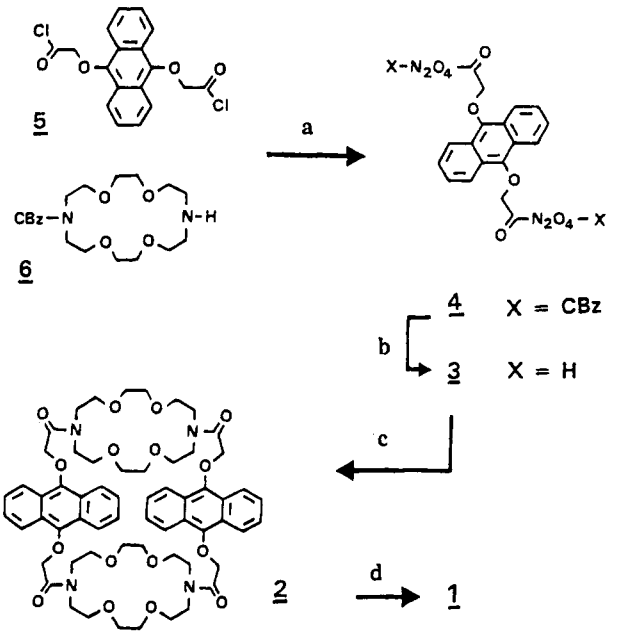

[a] (a) Et_3N, benzene; (b) HBr (30%), CH_3COOH. (c) **5**, Et_3N, benzene (high dilution). (d) i, B_2H_6, THF; ii, CF_3COOH, THF; iii, LiOH.

Synthesis of the Macrotricyclic Receptor 1

We used a stepwise procedure (Scheme 3) which involves the condensation of the monoprotected [18]-N_2O_4 **6**[13] with the diacid chloride **5**[14] to give the diamide **4**. Treatment of **4** with HBr/HOAc (33%) afforded the deprotected bis-macrocycle **3**, and condensation of **3** with the dichloride **5** at high dilution gave the macrotricyclic carboxamide **2** (45% yield). This tetraamide was reduced by diborane in tetrahydrofuran (THF) at reflux for about 10 h. Standard treatment of the crude amine–borane adduct (6 N HCl, either at reflux or at room temperature), which has been proven to be effective in the case of numerous related macropolycyclic compounds, failed here to afford the tetraamine **1**. This behavior is in opposition to that of a dibenzo analog[15] of **1**, and this is presumably due to the extreme sensitivity of the anthracene–oxygen bond toward acidic hydrolysis, giving rise to the formation of anthraquinone. Finally, the use of trifluoroacetic acid in refluxing THF under anhydrous conditions generated **1** in moderate yield. This synthesis was performed several times under these conditions leading to *ca.* 100 mg of **1** with an overall yield of *ca.* 5% (from **5**) in each run.

Compound **1** gave satisfactory analytical and spectral data, and, in particular, proton NMR spectroscopy fully confirmed the structure of **1** in $CDCl_3$ solution. In contrast to the ^1H NMR spectra of several anthracenocryptands,[4h,8] the absence here of any complex splitting pattern in the aliphatic region suggests the occurrence, in fluid solution at room temperature, of several conformers in rapid equilibration on the NMR time scale. Indeed, examination of Corey–Pauling–Koltun (CPK) models and a previous study[10] point to a high conformational flexibility of the receptor, presumably due to the

(11) Fages, F.; Desvergne, J.-P.; Bouas-Laurent, H.; Lehn, J.-M.; Konopelski, J.-K.; Marsau, P.; Barrans, Y. *J. Chem. Soc., Chem. Commun.* **1990**, 655.
(12) Bouas-Laurent, H.; Castellan, A.; Daney, M.; Desvergne, J.-P.; Guinand, G.; Marsau, P.; Riffaud, M.-H. *J. Am. Chem. Soc.* **1986**, *108*, 315.
(13) Lehn, J.-M.; Simon, J.; Wagner, J. *Nouv. J. Chim.* **1978**, *1*, 77.
(14) Hinschberger, J.; Desvergne, J.-P.; Bouas-Laurent, J.-P.; Marsau, P. *J. Chem. Soc., Perkin Trans. 2* **1990**, 993.
(15) Chapoteau, E.; Czerch, B. P.; Kumar, A.; Pose, A. *J. Incl. Phenom.* **1988**, *6*, 41.

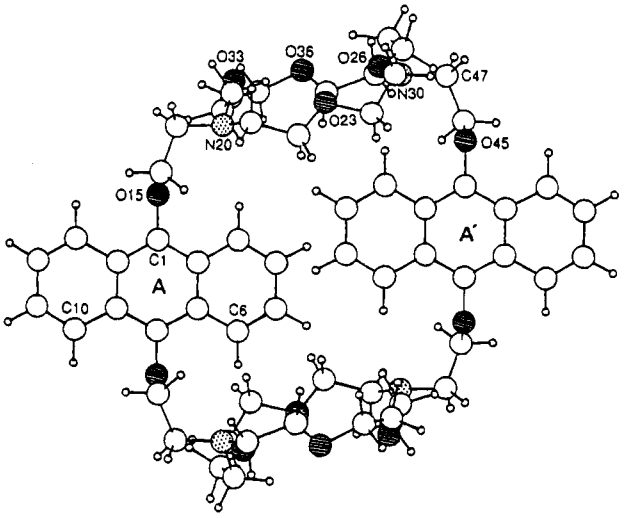

Figure 1. X-ray molecular structure of free receptor **1** (projection perpendicular to the aromatic planes A and A').

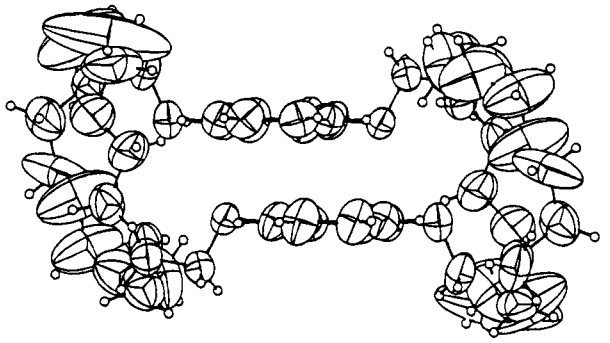

Figure 2. View of the free receptor **1** along the long axis of the anthracene units. Thermal ellipsoids are at 50% probability level, and H atoms are of arbitrary size. Large ellipsoids on the N_2O_4 ring are indicative of important disorder (see text).

presence of OCH_2CH_2 lateral linkages between the chromophores and the N_2O_4 subunits.

Structural Study of the Free Receptor

Projections of the molecular structure are given in Figures 1 and 2. Structural details about the N_2O_4 ring are less certain because of the disorder in atoms O(26), O(33), and O(36). This fact is indicative of the high flexibility of that part of the molecule even in the solid state, and therefore, Figure 1 shows a selected conformation. The solid-state structure of the free macrotricycle is centrosymmetric, and its overall shape is a cylinder presenting a flattened, central, hydrophobic cavity. Indeed, the two aromatic moieties, A and A', are contained in parallel planes 2.71 Å apart and displaced with respect to each other out of overlap. The arrangement of the anthracene groups, which tend to avoid each other, resembles that noticed in the free AA55 cyclophane[16] (Scheme 2), where the aromatic planes are separated by 3.04 Å. The N_2O_4 ring is rectangular shaped, the N atoms occupying roughly two opposite corners, and is almost perpendicular to the aromatic plane A (angle 79°). The four nitrogen bridgeheads are oriented toward the interior of the molecule, which should facilitate internal cation binding. Bond lengths and angles are found to be within normal limits, except for some values in the N_2O_4 macrocycle as expected from the above comments. Some intramolecular distances of interest for interchromophoric interactions are collected in Table 1.

(16) Marsau, P.; Bouas-Laurent, H.; Desvergne, J.-P.; Fages, F.; Lamotte, M.; Hinschberger, J. *Mol. Cryst. Liq. Cryst.* **1988**, *156*, 383.

Table 1. Selected Intramolecular Distances (Å) in the Solid State Structure of Free Macrotricycle 1 ($\sigma \leq 0.03$ Å)

N(20)···N(30)	6.99
N(20)···A(plane)[a]	−0.53
N(20)···A(center)[a]	5.29
N(20)···A(C(3))[a]	3.56
N(30)···A(plane)[a]	3.64
N(30)···A(center)[a]	10.45
N(30)···A'(C(6))[a]	3.55

[a] A and A' = anthracene groups (see Figure 1).

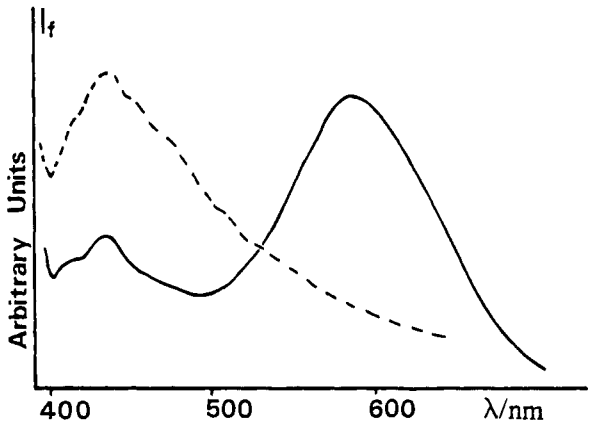

Figure 3. Fluorescence emission spectra of single crystals of free **1** (- - -) and of $[2Rb^+, \mathbf{1}]$, $2ClO_4^-$ (—) at room temperature (λ_{exc} = 380 nm); the long wavelength part peaking at 585 nm corresponds to the excimer emission, whereas the short wavelength emission is assumed to reflect the presence of some free ligand species located at defects.[20]

The single-crystal fluorescence spectrum of free receptor **1** displays a monomer-type emission (Figure 3) similar to that of free AA55, but the spectrum is significantly broadened and shifted to the red. From our previous studies[16] on bis-anthracenediyl cyclophanes and anthracenocryptands, we conclude that the intramolecular distances between aromatic nuclei are too long for intramolecular excimer formation. As the anthracene rings of two neighboring molecules are either located in parallel planes 6.02 Å apart, or oriented along (110) and $(1\bar{1}0)$ planes in a 86° herring-bone arrangement, the formation of intermolecular complexes can also be ruled out. The observed bathochromic shift with respect to AA55 could thus originate in intramolecular interactions between some nitrogen atoms and anthracene chromophores. Indeed, the shortest nitrogen−anthracene distances noticed in the structure of **1** (Table 1) are compatible with those allowing the formation of exciplex-type complexes.[16]

Crystal Structure of a Dinuclear Rubidium Cryptate

The structure of a crystalline complex between **1** and $RbClO_4$ is shown in Figures 4 and 5. Two complexed rubidium cations are located in the hydrophilic parts of the receptor, *e.g.* surrounded by the heteroatoms of the

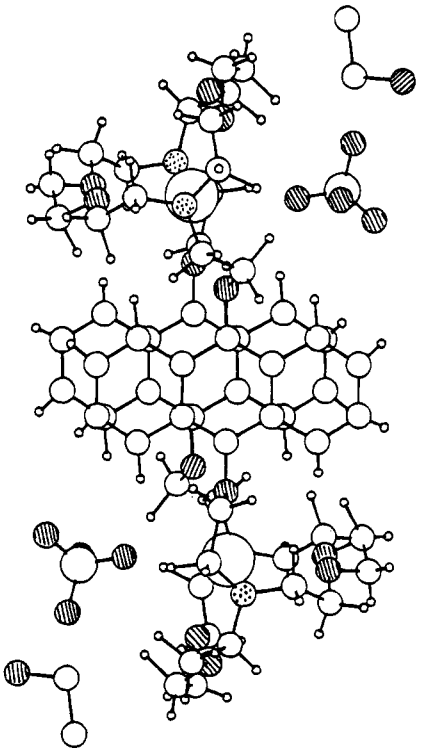

Figure 4. X-ray molecular structure of the rubidium dinuclear cryptate [$2Rb^+$, **1**], $2ClO_4^-$ (projection perpendicular to the aromatic planes).

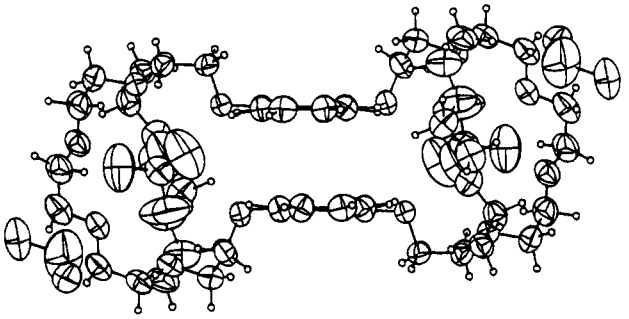

Figure 5. View of the dinuclear rubidium complex along the long axis of the anthracene units. Thermal ellipsoids are at 50% probability level, and H atoms are of arbitrary size. Large ellipsoids on the ClO_4^- anion and on the ethanol inclusion molecule reveal noticeable disorder. Upon complexation of Rb^+, N_2O_4 rings do not show any thermal disorder.

N_2O_4 rings and the four phenolic oxygens [O(15) and O(45)]. The classical mean plane of the diazacrown ether, defined by the four O-atoms and the two N-atoms, is not perpendicular to the major axis of the molecule (defined by the C(1)—C(8) direction), but makes an angle of about 52°. On the other hand, the mean plane of the atoms O(15), O(45), N(20), N(30), O(33), O(36) is quasi-parallel to that major axis (1.6° deviation). The ClO_4^- anion faces this plane with O(101) participating in the complexation of Rb^+. The ethanol of crystallization is located on the same side of the molecule as the ClO_4^- anion, but does not interact with the cation.

Finally, each Rb^+ is completely surrounded by nine heteroatoms (Figure 6). The corresponding distances are

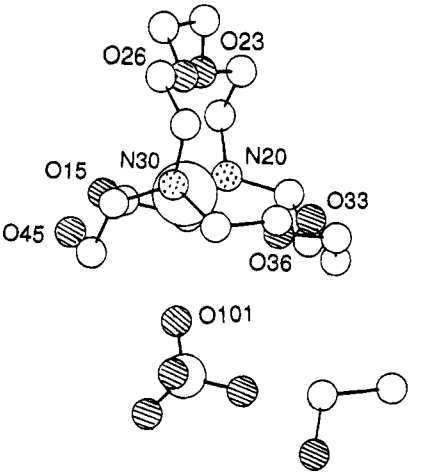

Figure 6. Part of the molecular structure showing the arrangement of the N and O atoms around the rubidium cation in the crystal and the ethanol inclusion molecule. Interestingly, the cations are surrounded by nine ligands which are at distances longer than the sum of the ionic radius of Rb^+ and the van der Waals radii of N and O heteroatoms (see Table 2).

Table 2. Intramolecular Distances (Å) between the Cryptated Rb^+ and the Coordinating Heteroatoms of the Receptor 1 and of the Perchlorate Anion (σ = 0.01 Å)[a]

Rb···N(20)	3.14	Rb···N(30)	3.14
Rb···O(23)	3.03	Rb···O(15)	2.98
Rb···O(26)	3.05	Rb···O(45)	3.07
Rb···O(33)	3.07		
Rb···O(36)	2.96	Rb···O(101)	2.95

[a] $r_i(Rb^+)$ = 1.48 Å. $r_{vdW}(N)$ = 1.50 Å. $r_{vdW}(O)$ = 1.40 Å.

listed in Table 2. They are quite longer than the sum of the ionic radius of Rb^+ (1.48 Å) and the van der Waals radii of nitrogen (1.50 Å) and oxygen (1.40 Å).[17] In the Rb^+ cryptate of Kryptofix 222,[18] Rb^+ is surrounded by the eight heteroatoms (six oxygen and two nitrogen atoms) and the heteroatom—metal distances were found close to the sum of the ionic and van der Waals radii. The occurrence of long distances indicates that the binding of Rb^+ to receptor **1** could be much better effected by an array of multiple weak interactions with a larger number of ligands. In agreement with this observation, O(101), even coordinated to the cation, has a thermal motion parameter of about 12 Å^2.

The presence of the two cations in the molecular cavity induces a slightly staggered sandwich conformation of the parallel (centrosymmetric) aromatic subunits: the interplanar separation is 3.46(4) Å, which corresponds to the van der Waals distance. The crystal fluorescence emission is represented in Figure 3; the broad red-shifted (λ_{max} = 585 nm) part of the spectrum is typical of a sandwich excimer fluorescence and resembles that observed for the sodium dinuclear complex of the AA55 cyclophane in the solid state;[19] the single crystal also exhibits a shorter wavelength emission (400–500 nm) which might presumably originate in free ligand species located in defect sites.[20]

(17) Pauling, L. *The Nature of The Chemical Bond*, 3rd ed.; Cornell University Press: Ithaca, New York, 1960.
(18) Metz, B.; Moras, D.; Weiss, R. *J. Chem. Soc., Chem. Commun.* **1970**, 217.
(19) Guinand, G.; Marsau, P.; Bouas-Laurent, H.; Castellan, A.; Desvergne, J.-P.; Lamotte, M. *Acta Crystallogr.* **1987**, *C43*, 857.
(20) Thomas, J. M.; Morsi, S. E.; Desvergne, J.-P. In *Advances in Physical Organic Chemistry*; Gold, V., Bethell, D., Eds.; Academic Press: London, 1977; Vol. 15, pp 64–131.
(21) Lehn, J.-M.; Sauvage, J.-P. *J. Am. Chem. Soc.* **1975**, *97*, 6700.

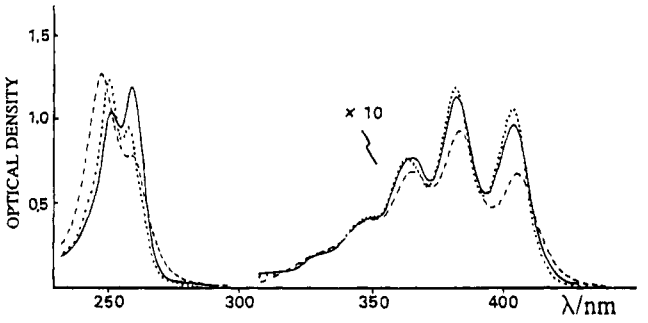

Figure 7. Electronic absorption spectra of **1** in methanol (conc *ca.* 10^{-4} M, 25 °C): (—) without salt; (···) with $NaClO_4$ (10^{-2} M); (- - -) with $RbClO_4$ (10^{-2} M).

Table 3. Changes in the UV Absorption Spectra of 1 (Conc *ca.* 10^{-4} M, CH_3OH, 25 °C) in the Presence of Alkali-Metal Cation Perchlorates (Conc *Ca.* 10^{-2} M)[a]

	^1B_b band				^1L_b band: 404 nm	
	251 nm		258 nm			
cation	$\Delta\epsilon$	$\Delta\lambda$	$\Delta\epsilon$	$\Delta\lambda$	$\Delta\epsilon$	$\Delta\lambda$
Na^+	↑17	–	↓20	←1	↑9	–
K^+	↑20	←1	↓17	–	↓7	–
Rb^+	↑20	←4	↓38	–	↓31	→1
Cs^+	↓4	←3	↓30	–	↓15	–

[a] $\Delta\epsilon$ represents the variation (%) of the molar absorption intensity and $\Delta\lambda$ the shift (nm). Arrows ↑ and ↓ denote hyper- and hypochromism, respectively. Arrows → and ← indicate batho- and hypsochromism, respectively. Dashes (–) indicate no effect.

Complexation and Photophysical Properties in Solution

UV–Visible Absorption Spectroscopy. The electronic absorption spectrum of **1** has been fully described in a previous paper.[10] It shows the spectral patterns characteristic of a series of cation-complexing anthracenophanes[12,14] due to some degree of overlap between the anthracenic chromophores, namely (i) hypochromic and bathochromic shifts in comparison with the spectrum of the monochromophoric compound (DMOA), (ii) a splitting of the high-energy absorption band located between 200 and 300 nm. The shape of the latter has been shown to be very sensitive to conformational changes occurring upon complexation of a substrate into the molecular cavity.

Unlike the absorption spectrum of DMOA, that of **1** is affected by the addition of alkali-metal cations perchlorates, the perturbation depending on the nature of the added species (Figure 7, Table 3). K^+, Rb^+, and Cs^+ give rise to common spectral changes that are consistent with an increase of the interactions between the aromatic parts. The largest amplitude of these effects is recorded with Rb^+. In contrast, the addition of Na^+ leads to opposite modifications of the low-energy band and to similar but less pronounced modifications of the high-energy band.

Fluorescence Emission. As depicted elsewhere,[10,11] the fluorescence emission spectrum of **1** in degassed methanol is dual and relatively weak in intensity as compared with that of the reference compound DMOA (Table 4). Indeed, beside the structured monomer-type region similar to DMOA emission, a broad and red-shifted band peaks at 530 nm and is ascribable to the formation of excimer-type intramolecular complexes ("excimer") resulting from the diverse interactions between, on one hand, the two anthracene rings and, on the other hand, the anthracene and the amino chromophores. Addition of salts to the methanolic solution of **1** was found to alter the emission spectrum selectively (Figure 8). In general, an increase of the total fluorescence intensity is observed (Table 4). The presence of K^+, Rb^+, and Cs^+ induces a red-shift of the "excimer" band and an enhancement of the intensity of that emission at the expense of the structured spectral part. The typical fluorescence emission recorded with Rb^+, which displays the highest Φ_{FE}/Φ_{FM} ratio, is indicative of the formation of a quasi-sandwich (slightly staggered) excimer. Fluorescence emission spectroscopy shows that Na^+ exhibits a peculiar behavior as compared to the other alkali-metal cations investigated, for it leads to the total disappearance of the excimer-type fluorescence. Under the same experimental conditions, no spectral modifications were detected with the monochromophoric reference compound DMOA.

From these experimental data, it is reasonable to admit that the effects of Rb^+ in solution are ascribable to the inclusion of two cations in the N_2O_4 complexation sites with an active participation of the phenolic-type oxygen to the stabilization of the structure. This is confirmed

Table 4. Fluorescence Quantum Yields of 1 and of 9,10-Dimethoxyanthracene (DMOA) in Degassed Methanol (Conc $<10^{-5}$ M, 25 °C, λ_{exc} = 380 nm) in the Absence and in the Presence of Alkali-Metal Cation Perchlorates (Conc *Ca.* 10^{-3} M)

	none	Na^+	K^+	Rb^+	Cs^+
DMOA	0.48	–	–	–	–
1 Φ_{FT}[a]	0.06	0.22[c]	0.21	0.24	0.21
Φ_{FM}[a]	0.03	0.22[c]	0.13	0.02	0.02
Φ_{FE}[a]	0.03	*d*	0.08	0.22	0.19
λ_{max}[b]	530	*d*	570	560	530

[a] Φ_{FT}, Φ_{FM}, and Φ_{FE} are total, monomer-like, and excimer-like fluorescence emission quantum yields, respectively. [b] Wavelength of the "excimer" emission maximum (nm). [c] Single fluorescence emission. [d] not observed. Dashes (–) indicate no effect.

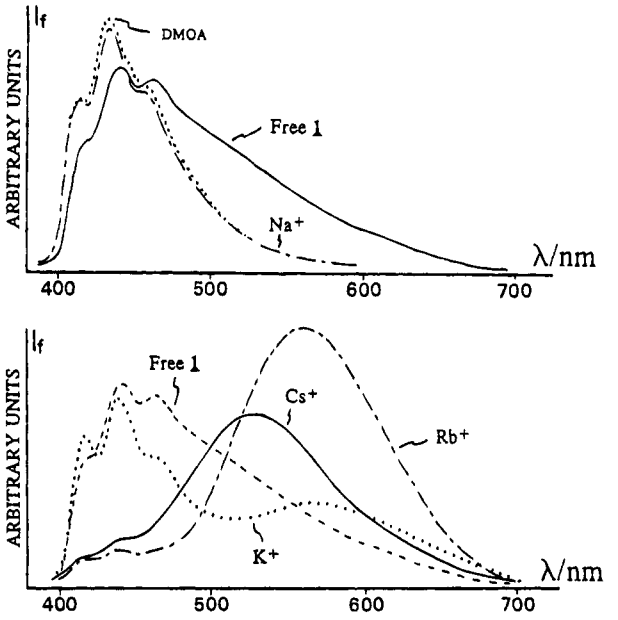

Figure 8. Corrected fluorescence emission spectra of **1** in degassed MeOH (conc $<10^{-5}$ M, 25 °C, λ_{exc} = 380 nm) in the absence and in the presence of alkali-metal cations (perchlorate salts, conc *ca.* 10^{-3} M).

(22) Sillen, L. G.; Warnquist, B. *Arkiv. Kemi.* **1968**, *31*, 315; 377.
(23) Lehn, J.-M.; Simon, J. *Helv. Chim. Acta* **1977**, *60*, 141.

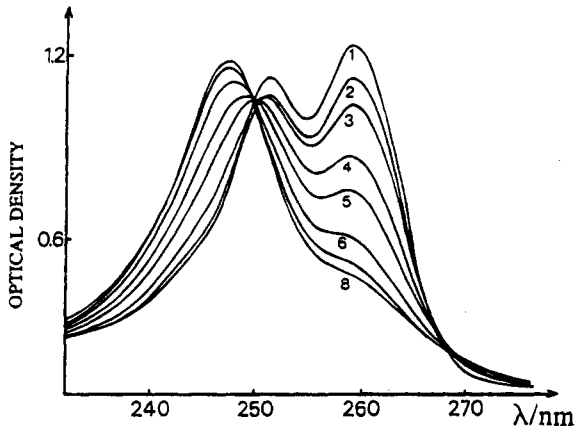

Figure 9. Spectrophotometric titration of ligand **1** by $RbClO_4$ ($CH_3OH/CHCl_3$ 98/2 (v/v); 25 °C). $[\mathbf{1}]_0 = 9.21 \times 10^{-6}$ M. $[Rb^+]_0 \times 10^6$ M: 1, 0.0; 2, 4.61; 3, 9.21; 4, 18.4; 5, 27.6; 6, 55.3; 7, 82.9; 8, 166.

by the determination of the stability constants of the rubidium complexes (*vide infra*). The fluorescence emission of **1** in the presence of a large excess of $RbClO_4$ in solution is quite similar to that of the crystal and therefore the crystal and solution structures of the rubidium dinuclear complexes should be the same. Furthermore, ^1H NMR[11] and UV absorption data confirm the ground-state structure in solution, in which the two aromatic rings are parallel and close together. From similar spectroscopic trends, it can be assumed that **1** forms with K^+ and Cs^+ binuclear cryptates exhibiting similar structural features in solution.

On the other hand, it might well be that the sodium cations are held by the N_2O_4 macrocycles without any noticeable participation of the phenolic oxygens. Such participation would require a pronounced contraction of the complexing cavities around these smaller cations, thus introducing steric repulsions, as was observed[21] for the [3.2.2] cryptand. In the case of **1**, this destabilizing effect would be more pronounced due to the presence of the bulky anthracene units. From examination of the UV absorption spectra, one can suppose that, in binding Na^+ cations, receptor **1** forms a complex in which the two anthracenes hold their long axes parallel, but not their short ones. Thus, no sandwich interaction or significant overlap leading to excimer emission would occur.

Determination of the Stability Constants of the Rubidium Complexes. Spectrophotometric titrations of ligand **1** by $RbClO_4$ were performed in the $CH_3OH/CHCl_3$ (98/2, v/v) solvent system at room temperature. After each addition, the absorption spectrum was recorded between 230 and 280 nm (Figure 9). The data were processed with the nonlinear regression program LETAGROP-SPEFO.[22] The best statistical fit has been obtained for the formation of 1/1 and a 2/1 rubidium/receptor complexes. The distribution diagram (Figure 10a) shows the disappearance of the free ligand for a metal-to-ligand concentration ratio of about 6. The maximal proportion (60%) of mononuclear complex is achieved when the ratio is 1.5.

The stability constants of these two complexes and those published[23] for macrotricyclic ligands **7**–**9** are collected in Table 5. Two main features emerge from the comparison of these data: (i) the stability constants K_1 and K_2 determined for **1** are 2 order of magnitudes higher than those reported for **7**–**9**; (ii) $\Delta(\log K)$ (= $\log K_1 - \log K_2$) is larger in the case of molecule **1** than in the cases of **7**–**9**.

The use of different experimental conditions (*e.g.* solvent systems of higher polarity and Cl^- as counteranion) might, to a large extent, account for explain the lower K_1 and K_2 values obtained in the previous studies. In our case, the gain in stability could also be due to the presence, in receptor **1**, of the four oxygens, in the 9,10-positions of the anthracene units, which have been shown to interact with the two Rb^+ cations. These interactions are likely to bring some degree of stabilization to the complexes, as compared to ligands **7** and **8**. Indeed, **9**, bearing two oxygen atoms in the lateral bridges, shows a slightly better affinity for Rb^+ than do **7** and **8**.

In the case of **1**, the value of 0.98 obtained for $\Delta(\log K)$ indicates that the 2/1 complex is 1 power of 10 less stable than the 1/1 complex. If the two complexing sites were totally independent, statistical factors[24] alone would result in $K_1/K_2 = 4$ and $\Delta(\log K) = 0.6$. If one considers that mere electrostatic repulsion of two charges is the only factor destabilizing the binuclear complex with respect to the 1/1 complex according to Lehn and Simon,[23] one should obtain $\Delta(\log K) = 0.78$ for a $Rb^+ \cdots Rb^+$ distance of about 9.75 Å, in the case of receptor **1**; in comparison $\Delta(\log K)$ would amount to 1.1 for the distance of about 6–7 Å, in ligands **7**–**9**.[23] The experimental $\Delta(\log K)$ values obtained for **7**–**9** are much lower than 1.1

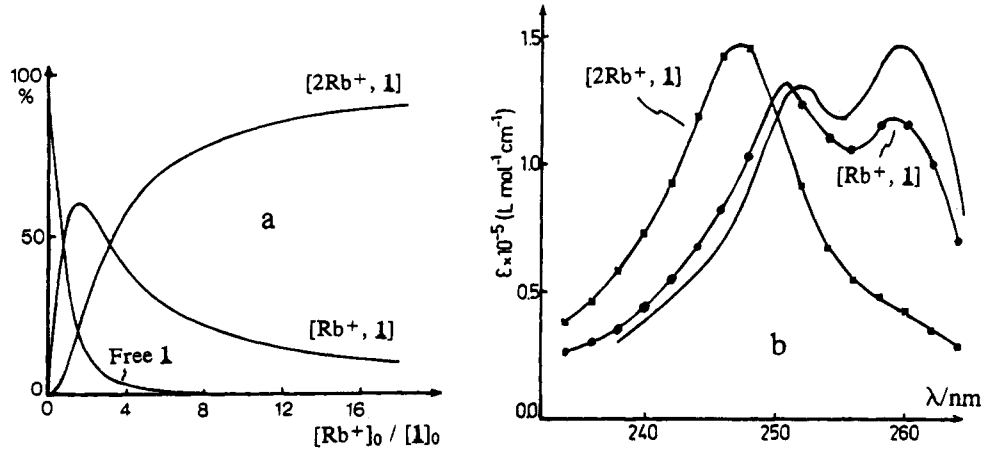

Figure 10. Distribution diagram (a) of free **1**, [Rb^+, **1**], and [2Rb^+, **1**], and calculated electronic absorption spectra (b) of the complexes: (—) experimental spectrum of free **1** ($CH_3OH/CHCl_3$ 98/2 (v/v); 25 °C, $[\mathbf{1}]_0 = 9.21 \times 10^{-6}$ M).

Table 5. Stability Constants Determined for the Rubidium Complexes of 1 and Published Data for Related Macrotricycles[a]

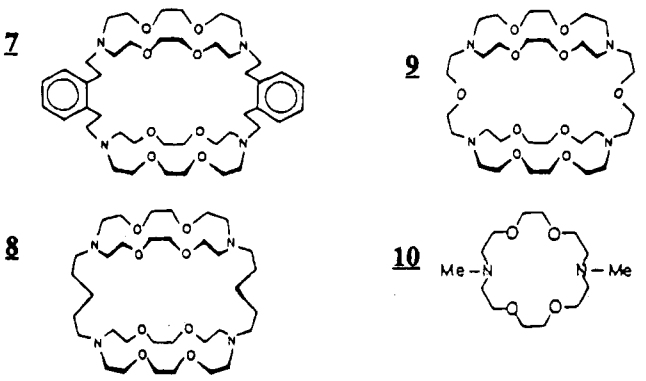

ligands:	1[b]	7[c]	8[c]	9[c]	10[d]
$\log K_1$	5.78 ± 0.08	3.0 ± 0.2	3.5 ± 0.2	3.7 ± 0.2	4.3 ± 0.2
$\log K_2$	4.8 ± 0.2	2.8 ± 0.4	3.0 ± 0.4	3.3 ± 0.4	–

[a] The uncertainity values correspond to the estimated experimental errors (K_1 and K_2 in L mol^{-1} at 25 °C). [b] $CH_3OH/CHCl_3$ 98/2 (v/v). [c] CH_3OH/H_2O 95/5 (v/v); $I = 0.1$; nitrate as counteranion. See ref 23. [d] CH_3OH; $I = 0.01$; chloride as counteranion. See ref 21.

(the largest being 0.5); indeed, ligands **7**–**9** (Table 5) were shown to contain two almost independent macrocyclic sites. If it were the case for the longer ligand, **1**, one would expect $\Delta(\log K) \leq 0.5$. In fact, an additional destabilization has to be taken in account in the case of **1**, which could originate in residual interactions between the π clouds of the aromatic nuclei. Indeed, in the binuclear complex [2Rb$^+$, **1**], the participation of the phenolic oxygen atoms induces the formation of a structure in which the anthracene chromophores overlap and are enforced to keep a ground-state interplanar separation close to the van der Waals distance. Finally, a noncooperative behavior is observed.

Figure 8b shows the calculated UV absorption spectra of [Rb$^+$, **1**] and [2Rb$^+$, **1**]. The complexation of the second cation dramatically alters the spectrum of **1** and is indicative of the increased degree of interaction between the anthracenes.

Conclusion

We have prepared a macrotricyclic ligand which displays a dual fluorescence (monomer and excimer-like) emission. The fluorescence of that compound is highly sensitive to the presence of alkali-metal cations and is dependent on the nature of the complexed species. A spectacular effect is noticed in the presence of Rb$^+$, and this is the first example of fluorescence detection of this cation.

Experimental Section

Chemicals and Solvents. All reagents and solvents (spectrometric grade) were purchased commercially and used without further purification, except as below. Benzene was distilled from calcium hydride. THF was refluxed with and distilled from sodium benzophenone ketyl. Triethylamine was distilled from KOH pellets and stored over 4-Å molecular sieves. The N-benzyloxycarbonyl (CBz) monoprotected [18]-N_2O_4 macrocycle[13] **6**, DMOA (9,10-dimethoxyanthracene),[25] and the diacid chloride[14], **5** [(anthracene-9,10-diyldioxy)bis(acetylchloride)], were synthesized according to known procedures.

Thin-layer chromatography was performed on aluminum-backed 0.2-mm E. Merck precoated silica gel plates (60 F-254) or aluminum oxide plates (60 F-254 neutral type E). Column chromatography was performed on neutral alumina (Brockmann I, 150 mesh, standard grade) obtained from Aldrich. Alkali-metal perchlorates were of analytical grade. All the anthracene derivatives were treated as if they were light- and oxygen-sensitive; the reactions were therefore performed in degassed solvents, under an inert atmosphere (nitrogen or argon), and in the dark.

Physical and Spectroscopic Methods. Melting points were measured on a Kofler block and are uncorrected. IR and UV spectra were recorded on a Perkin-Elmer model 412 instrument and on a Cary 219 spectrophotometer, respectively. Proton NMR were recorded on either a Perkin-Elmer R-24B (60 MHz) or a Bruker AC 250 (250 MHz). Chemical shifts are reported in ppm *vs* Me_4Si. Mass spectrometry was performed with a VG analytical Autospec-Q in the fast-atom bombardment (FAB) mode. Microanalyses were obtained at the Service Central d'Analyse du CNRS, Vernaison, France. Fluorescence spectra were obtained with a Hitachi Perkin-Elmer 44 or a Spex Fluorolog, and are corrected for emission. The fluorescence quantum yields were determined on degassed samples by comparison with quinine sulfate in 1 N sulfuric acid.[26] Degassing was carried out on a high-vacuum line using repeated freeze–pump–thaw cycles. All the measurements were performed at room temperature (25 °C).

Anthracene-Bridged Bis-[18]-N_2O_4 Macrocycle 3. Step 1: Preparation of 4. To a solution of the *N*-benzyloxycarbonyl monoprotected [18]-N_2O_4 macrocycle[13] **6** (3 g; 7.6 mmol) and triethylamine (3 mL) in benzene (100 mL) was added a solution of **5**[14] (1.30 g; 3.6 mmol) in benzene (100 mL) over a period of 4 h, under a nitrogen atmosphere, and with vigorous stirring. After the reaction mixture was washed with 100 mL of 10% aqueous NaOH, the organic layer was dried over Na_2SO_4 and evaporated to dryness to yield the diprotected diamide **4** as an oil (3.80 g; quantitative). This product was used directly without further purification: ^{1}H NMR ($CDCl_3$) 3.5, 4.85, 5.05, 7.3, 7.45–8.30 ppm; IR (NaCl film) 3060, 3040, 3000, 2844, 1685, 1640, 1450, 1400, 1380, 1340, 1220, 1100, 1060, 1020, 900, 760, 690, 680 cm^{-1}.

Step 2: Preparation of 3. The diprotected diamide **4** (3.80 g) was treated with 50 mL of HBr in acetic acid (33%) at room temperature for 4 h. Distilled water (150 mL) was then added and the mixture was extracted with 3 × 200 mL of $CHCl_3$. The aqueous layer was made alkaline by addition of NaOH (30%) and extracted with 3 × 200 mL of $CHCl_3$. These last chloroform extracts were combined, dried (Na_2SO_4), and evaporated to give a viscous yellow oil. Chromatography of the crude oil on alumina (CH_2Cl_2 as eluent) gave **3** as a pale yellow waxy product (1.80 g, 61% yield): ^{1}H NMR ($CDCl_3$) 2.65, 4.5, 4.85, 7.50–8.30 ppm; IR (NaCl film) 3300, 2990, 2850, 1640, 1450, 1340, 1300, 1280, 1240, 1120, 1070, 780, 750 cm^{-1}.

Bis-Anthracene Bis-[18]-N_2O_4 Macrocyclic Tetraamide 2. A solution of diamine **3** (1.80 g, 2.2 mmol) and triethylamine (2 mL) in benzene (500 mL) and a solution of diacid chloride[14] **5** (0.80 g, 2.2 mmol) in benzene (500 mL) were simultaneously added dropwise to 2 L of benzene under nitrogen atmosphere and vigorous stirring. The addition required about 7 h. After evaporation of the solvent, the residue was dissolved in $CHCl_3$ (200 mL) and this solution was successively extracted with (i) 3 × 100 mL of hydrochloric acid (10%), (ii) 3 × 100 mL of sodium hydroxide (10%), and (iii) distilled water up to neutral pH. The organic phase was then dried ($MgSO_4$) and evaporated to give a brownish solid which was chromatographed on alumina [CH_2Cl_2/MeOH, 98:2 (v/v)]. Tetraamide **2** (1.10 g, 45% yield) was obtained as a pale yellow solid: mp 226–230 °C; ^{1}H NMR ($CDCl_3$) 3.00–4.00, 4.85, 7.00–8.30 ppm; IR (KBr

(24) Perlmutter-Hayman, B. *Acc. Chem. Res.* **1986**, *19*, 90.

(25) Meyer, K. H. *Justus Liebig's Ann. Chem.* **1911**, *379*, 70.

(26) Hanai, S.; Hirayama, F. *J. Phys. Chem.* **1983**, *87*, 83 and references therein.

Table 6. Crystal and Experimental Data for 1 and [2Rb$^+$, 1], 2ClO$_4^-$

	1	[2Rb$^+$, 1], 2ClO$_4^-$
formula	$C_{60}H_{80}N_4O_{12}$	$C_{60}H_{80}N_4O_{12}$, $2RbClO_4$
fw	1049.31	1419.15
crystal size, mm	0.15 × 0.25 × 0.40	0.4 × 0.4 × 1.0
system	monoclinic	triclinic
space group	$P2_1/n$	P_1
a, Å	13.428(2)	13.089(1)
b, Å	11.623(4)	13.166(1)
c, Å	19.377(3)	13.824(1)
α, deg		105.15(1)
β, deg	107.45(3)	94.99(1)
γ, deg		126.97(1)
V, Å^3	2885	1742.7
Z	2	1
total data	4803	6582
observed data ($I > 3\sigma(I)$)	2258	4612
R	0.076	0.069

pellet) 2820, 2760, 1640, 1460, 1430, 1380, 1345, 1300, 1230, 1160, 1120, 1080, 1020, 770, 680 cm^{-1}; MS (FAB$^+$, glycerol) 1105 (calcd 1105). Anal. Calcd for $C_{60}H_{72}N_4O_{16}\cdot 2H_2O$ (dihydrate): C, 63.16; H, 6.67; N, 4.91; O, 25.26. Found: C, 63.65; H, 6.51; N, 4.67; O, 25.43.

1,7,10,16,17,23,26,32,35,38,43,46,-dodecaoxa-4,13,20,29-tetraaza-[16.8^{4,13}.16.8^{20,29}](9,10)-anthracenophane (1).[28] Diborane (20 mL of a 1 M solution in THF) was added to a suspension of tetraamide **2** (0.55 g, 0.5 mmol) in THF (20 mL) at 0 °C under an argon atmosphere. The resulting mixture was heated at reflux for 10 h. After the mixture was cooled, the excess diborane was cautiously quenched with water. The reaction mixture was then taken to dryness on a rotary evaporator. The resulting solid residue was suspended in THF (20 mL), trifluoroacetic acid (20 mL) was slowly added, and the mixture was heated at reflux for 2 h under an argon atmosphere. After being cooled, the solution was brought to pH 10 or 11 by the addition of aqueous LiOH (30%) and was extracted with $CHCl_3$ (3 × 100 mL). The combined organic extracts were dried over $MgSO_4$ and evaporated to dryness. The crude product was chromatographed on alumina, eluting with 2% CH_3OH in CH_2Cl_2, to yield, after recrystallization from CH_2Cl_2–CH_3OH, 100 mg of the tetraamine **1** (19% yield): mp 211–2 °C; ^{1}H NMR ($CDCl_3$) 2.92, 3.14, 3.66, 3.71, 4.17, 7.32–8.37 ppm; IR (KBr pellet) 2930, 2860, 1620, 1400, 1380, 1340, 1120, 1070, 780, 760 cm^{-1}; high-resolution MS (FAB$^+$, glycerol) 1049.5831 (calcd for $C_{60}H_{80}N_4O_{12}$ +1H, 1049.5851). Anal. Calcd for $C_{60}H_{80}N_4O_{12}\cdot 1.5H_2O$: C, 66.98; H, 7.72; N, 5.21. Found: C, 67.16; H, 7.48; N, 5.07.

X-ray Structural Determinations. X-ray measurements were performed at room temperature on a CAD4 Enraf-Nonius diffractometer using a graphite-monochromatized Cu K$_\alpha$ (λ = 1.5418 Å) radiation. Full details of the structure determinations are available as supplementary material.

Structure of the Free Ligand. In an attempt to grow crystals of the α,ω-diammonium complex of **1**, good crystals of free **1** were unexpectedly obtained from the slow evaporation of a solution of **1** and an equimolar amount of α,ω-hexamethylenediammonium dipicrate in a chloroform–methanol–toluene solvent system. A yellow needle was subjected to X-ray diffraction, and lattice parameters were determined from 25 reflections by least-squares refinement. The crystallographic data are collected in Table 6. The structure was solved by direct methods[27] and the number of non-H atoms localized was extended from 22 to 32 in three steps. In the refinement, by block-diagonal least-squares method with a local program, isotropic thermal B_i coefficients were used; some of the coefficients in the N_2O_4 rings showed rather large values. Hydrogen atoms were progressively introduced in theoretical positions before the application of anisotropic thermal coefficients to the well-localized non-H atoms. Differential Fourier synthesis did not show any inclusions and the sections of electronic density presented diffuse zones corresponding to atoms with large B_i values that were part of the N_2O_4 group. Conformations having all these atoms in limit positions could neither be well defined nor refined. The calculations were achieved with the dubious atoms O(26), O(33), and O(36) in mean positions with high values of anisotropic thermal coefficients, which reflects important delocalization (the corresponding bond lengths and angles are not significant). The H atoms were refined in the ultimate step. The residual densities are less than 0.5 e$^-$/Å^3.

Structure of the Rubidium Dinuclear Cryptate. The crystal was obtained as a yellow needle from a chloroform–methanol–ethanol solution of **1** in presence of a large excess of $RbClO_4$. A first account of the structure has been already reported.[11] The final structure and additional details about the solvent inclusion are given therein. Lattice parameters were determined from 21 reflections by least-squares refinement, and the crystallographic data are given in Table 6. The structure was solved by the Patterson method. Refinement was carried out by using a block-diagonal least-squares method with anisotropic thermal parameters for non-H atoms. All hydrogen atoms (except on the solvent of inclusion) were introduced at calculated positions and refined with isotropic thermal parameters. At this step, Fourier difference maps showed residual densities identified as a molecule of ethanol, affected by disorder essentially on the central atom, C(300). The largest motion is orthogonal to the mean plane O(304)–C(300)–C(305). The ClO_4^- anions are also affected by some disorder of the O atoms, whose thermal parameters B_{eq} are between 12 and 18 Å^2. In contrast, the central Cl atoms are well defined, with B_{eq} = 6.6 Å^2, so that the quasi-spherical perchlorate anions rotate around the respective central chlorine atoms. All bond distances are in good agreement with values generally admitted, except for the ethanol inclusion molecules and the perchlorates anions. No residual final densities were found higher than 0.5 e$^-$/Å^3.

Acknowledgment. La Région Aquitaine is thanked for partial support for the equipment of the CESAMO (Centre d'Etude de la Structure et d'Analyse des Molécules Organiques). The CNRS and the University Bordeaux I are gratefully acknowledged for financial assistance. We appreciate the expertise of Dr. G. Bourgeois (CESAMO) in mass spectrometry, and we thank J.-P. Konopelski for initial studies on the synthesis of ligand **1**.

Supplementary Material Available: Complete crystallographic details (14 pages). This material is contained in libraries on microfiche, immediately follows this article in the microfilm version of the journal, and can be ordered from the ACS; see any current masthead page for ordering information.

(27) Gilmore, C. J. *J. Appl. Crystallogr.* **1984**, *17*, 42.

(28) The author has deposited atomic coordinates for this structure with the Cambridge Crystallographic Data Centre. The coordinates can be obtained, on request, from the Director, Cambridge Crystallographic Data Centre, 12 Union Road, Cambridge, CB2 1EZ, UK.